Acta Crystallographica Section D
Biological Crystallography
ISSN 1399-0047

Structural basis for the selective nuclear import of the C2H2 zinc-finger protein Snail by importin β

Saehae Choi,[a] Eiki Yamashita,[b] Noriko Yasuhara,[c,d] Jinsue Song,[a] Se-Young Son,[a] Young Han Won,[a] Hye Rim Hong,[a] Yoon Sik Shin,[a] Toshihiro Sekimoto,[d] Il Yeong Park,[a] Yoshihiro Yoneda[c,d,e]* and Soo Jae Lee[a]*

[a]College of Pharmacy, Chungbuk National University, Seungbong 410, Heungduk, Cheongju, Chungbuk 361-763, Republic of Korea, [b]Institute for Protein Research, Osaka University, 1-3 Yamada-oka, Suita, Osaka 565-0871, Japan, [c]Department of Frontier Biosciences, Graduate School of Frontier Biosciences, Osaka University, 1-3 Yamada-oka, Suita, Osaka 565-0871, Japan, [d]Department of Biochemistry, Graduate School of Medicine, Osaka University, 1-3 Yamada-oka, Suita, Osaka 565-0871, Japan, and [e]JST, CREST, Graduate School of Frontier Biosciences, Osaka University, 1-3 Yamada-oka, Suita, Osaka 565-0871, Japan

Correspondence e-mail: yyoneda@anat3.med.osaka-u.ac.jp, sjlee@chungbuk.ac.kr

Received 29 October 2013
Accepted 14 January 2014

PDB reference: Snail1–importin β complex, 3w5k

Snail contributes to the epithelial–mesenchymal transition by suppressing E-cadherin in transcription processes. The Snail C2H2-type zinc-finger (ZF) domain functions both as a nuclear localization signal which binds to importin β directly and as a DNA-binding domain. Here, a 2.5 Å resolution structure of four ZF domains of Snail1 complexed with importin β is presented. The X-ray structure reveals that the four ZFs of Snail1 are required for tight binding to importin β in the nuclear import of Snail1. The shape of the ZFs in the X-ray structure is reminiscent of a round snail, where ZF1 represents the head, ZF2–ZF4 the shell, showing a novel interaction mode, and the five C-terminal residues the tail. Although there are many kinds of C2H2-type ZFs which have the same fold as Snail, nuclear import by direct recognition of importin β is observed in a limited number of C2H2-type ZF proteins such as Snail, Wt1, KLF1 and KLF8, which have the common feature of terminating in ZF domains with a short tail of amino acids.

1. Introduction

The change of cell mobility in the epithelial–mesenchymal transition (EMT) is an important developmental process (Thiery, 2002; Thiery & Sleeman, 2006; Peinado *et al.*, 2007). Snail participates in the EMT concerning the formation of mesoderm and neural crest during embryonic development (Cano *et al.*, 2000; Batlle *et al.*, 2000). Emerging evidence shows that Snail is a key factor in metastasis in melanoma, bladder, colorectal and pancreatic carcinomas (Cano *et al.*, 2000; Batlle *et al.*, 2000; Poser *et al.*, 2001; De Craene *et al.*, 2005). In these tumours, the down-regulation of E-cadherin has been observed to correlate with the high-level expression of Snail. Thus, Snail contributes to EMT by suppressing E-cadherin, which is thought to be a suppressor of invasion during cancer metastasis. Among vertebrates, the Snail family is divided into three members, Snail1, Snail2 and Snail3, each of which are zinc-finger (ZF) transcription factors. The Snail family members are composed of a highly conserved C-terminal region containing four to five adjacent C2H2-type ZF domains, an N-terminal SNAG domain and a divergent central region (Peinado *et al.*, 2007). The zinc fingers function as DNA-binding domains that recognize consensus E2-box-type elements (Klug, 2010). Recently, the zinc finger was also found to function as a nuclear localization signal (NLS), and Snail1 can be transported into the nucleus in an importin β-mediated manner (Sekimoto *et al.*, 2011; Mingot *et al.*, 2009). The conserved SNAG domain, composed of 7–9 amino acids in the N-terminus of the protein, is responsible for the repressor capacity (Peinado *et al.*, 2004). The central region of the Snail protein contains a serine/proline-rich region which is highly divergent between Snail members. Two different

functional domains have been identified in the central region of the Snail1 protein: a regulatory domain containing a nuclear export signal (NES; Domínguez *et al.*, 2003) and a destruction-box domain (Zhou *et al.*, 2004). Phosphorylation of the Snail1 destruction box, creating a recognition site for β-TrCP, is critical for post-translational regulation, which induces the degradation of the protein by the ubiquitin–proteasome system (Zhou *et al.*, 2004). Nuclear export by exportin 1 is facilitated by serine phosphorylation of Snail1 (Domínguez *et al.*, 2003; Wu *et al.*, 2009), whereas dephosphorylated Snail is present only in the nucleus to enhance its activity (Wu *et al.*, 2009). Glycogen synthase kinase 3β (GSK3β) and p21-activated kinase (Pak1) have been identified as kinases for this phosphorylation of Snail (Zhou *et al.*, 2004; Yang *et al.*, 2005). Control of the nucleo-cytoplasmic localization of Snail is crucial for its activity.

Transport of macromolecules such as proteins and RNAs through the nuclear pore complex (NPC) is mediated by the soluble transport factors importins and exportins, which bind to NLSs and NESs in their respective cargo molecules. Importin β family proteins recognize a variety of NLSs directly or indirectly to transport macromolecules into the nucleus through the NPC *via* transient interactions with phenylalanine–glycine (FG) repeat-containing nucleoporins (Stewart, 2007). As NLS receptors, importin α family proteins form the NLS–importin α binary complex by recognition of the classical basic NLS-containing proteins. The binary complex is bound to importin β to form an NLS–importin α–importin β ternary complex, which is then translocated through the NPC into the nucleus. Previous results have shown that importin β mediates the nuclear import of Snail1 through direct binding to its ZF domains (Sekimoto *et al.*, 2011; Yamasaki *et al.*, 2005; Mingot *et al.*, 2009). Also, it has recently been shown that other importin β family members, importin 7 and transportin, are also involved in nuclear transport of Snail1 (Mingot *et al.*, 2009). Although there are many kinds of C2H2-type ZF structures which have the same motif as Snail, nuclear import by direct recognition of importin β is observed in only a limited number of C2H2-type ZF proteins (Yamasaki *et al.*, 2005; Mingot *et al.*, 2009; Depping *et al.*, 2012). Here, we report the structure of a Snail1 ZF domains–importin β complex at 2.5 Å resolution. The results provide structural details of the novel interactions between the Snail1 ZF domains and importin β. Furthermore, the binary-complex structure explains how importin β differentiates the specific C2H2 ZF domains of Snail1 from those of other structurally similar C2H2 ZF proteins.

2. Materials and methods

2.1. Cloning

Full-length human importin β was amplified by PCR with primers containing *Nde*I and *Xho*I restriction-enzyme sites and was subcloned into pET28-Tev vector. The ZF region of the human Snail1 fragment was constructed by cloning residues 153–264 into the *Bam*HI and *Sal*I sites of the pGEX4T-Tev vector. Point mutants of Snail1 were generated using the Muta direct site-directed mutagenesis kit (Intron) with primers designed to change the amino acid. Single mutations were induced where each complementary primer changed one or both DNA sequences, and the mutated residues were as follows: R191E, W193A, Q196A, R224E, Q228A, R243E, R247E and K253E. Mutations which changed two or more amino acids were performed through site-directed mutagenesis with the confirmed primary mutant plasmid. Snail1 C-terminal deletion (residues 153–261) and ZF(2–4) (residues 180–264) mutants were amplified using primers designed to introduce a stop codon at position 261 and a start codon at position 179, respectively. The Snail1 GFP mutant was subcloned into pGEX4T-GFP, which contains GFP between *Sma*I and *Eco*RI in the C-terminus. All constructs were confirmed by sequence analysis (Solgent).

2.2. Expression and purification

Importin β and Snail zinc-finger domains were expressed in *Escherichia coli* strain BL21 (DE3) and were grown for 2 h at 37°C (A_{600} = 0.5) in 2×YT medium. Importin β expression was induced with 1 m*M* isopropyl β-D-1-thiogalactopyranoside (IPTG) at 20°C overnight, and Snail1 was induced with 0.5 m*M* IPTG, 1 m*M* $ZnCl_2$ at 25°C for 5 h. The cells were harvested by centrifugation at 6000 rev min^{-1} for 10 min at 4°C and were stored at −80°C. Cells expressing importin β and Snail1 were mixed, resuspended in 20 m*M* Tris–HCl pH 7.4, 300 m*M* NaCl, 1 m*M* dithiothreitol (DTT), 0.1 m*M* PMSF and were lysed by sonication on ice. After centrifugation at 18 000 rev min^{-1} for 40 min, the supernatant was loaded onto phenyl Sepharose (GE Healthcare) and was eluted with distilled water. The eluted sample was added to the same volume of 20 m*M* Tris–HCl pH 7.4, 300 m*M* NaCl, 1 m*M* DTT and was then purified with Glutathione Sepharose 4 Fast Flow beads (GE Healthcare). This sample was then incubated with TEV protease at 20°C overnight; to separate the GST tag, the sample was loaded onto Phenyl Sepharose beads and eluted with distilled water. The complex was finally purified on a Superdex 200 (Amersham Biosciences) gel-filtration column which was pre-equilibrated with 20 m*M* Tris–HCl pH 7.4, 1 m*M* DTT.

2.3. Crystallization and data collection

The importin β–snail ZF domains complex was concentrated to 30 mg ml^{-1} using a centrifugal concentrator (Sartorius) and was filtered with a centrifugal filter (Millipore). Crystallization was performed by the hanging-drop vapour-diffusion method using a 2 µl drop consisting of equal volumes of protein and precipitation buffer [0.1 *M* bis-tris–HCl pH 6.7, 11.5%(*w*/*v*) PEG 8000, 0.5 *M* urea]. 7.5%(*v*/*v*) glycerol and 0.5 CMC (critical micelle concentration) of nonyl-β-D-glucoside (final concentration) were added to the 2 µl drop, which was equilibrated against 400 µl reservoir solution with the addition of 15%(*v*/*v*) glycerol at 20°C. The detailed purification and crystallization methods are described in Choi *et al.* (2013). The cryoprotectant solution for cooling

Table 1
Crystallographic and refinement statistics for the human Snail1 ZF–importin β complex.

Values in parentheses are for the highest resolution shell.

		Phasing		
	High resolution	Peak	Inflection	Remote
Data collection				
Space group	*C*2	*C*2		
Unit-cell parameters				
a (Å)	228.21	234.06		
b (Å)	77.53	75.63		
c (Å)	72.02	72.65		
α (°)	90.0	90.0		
β (°)	100.9	102.0		
γ (°)	90.0	90.0		
Wavelength (Å)	0.900	1.2823	1.2831	1.2571
Resolution (Å)	2.5	3.5	3.8	3.9
R_{merge}	0.064 (0.415)	0.075 (0.416)	0.119 (0.541)	0.116 (0.474)
$\langle I/\sigma(I)\rangle$	34.7 (5.4)	33.7 (4.2)	39.6 (9.1)	40.7 (10.5)
Completeness (%)	97 5 (99.2)	99.7 (100)	98.8 (100)	98.9 (100)
Multiplicity	4.1 (4.0)	7.4 (7.5)	5.6 (6.0)	5.7 (6.0)
Refinement				
Resolution (Å)	2.5			
No. of reflections	41582			
R_{work}/R_{free}	0.225/0.268			
No. of atoms				
Total	7593			
Protein	7542			
Ligand/ion	0/4			
Water	47			
B factors (Å^2)				
Overall	77.6			
Protein				
Importin β	74.8			
Snail	99.2			
Water	64.6			
R.m.s. deviations				
Bond lengths (Å)	0.0052			
Bond angles (°)	0.897			
Ramachandran plot (%)				
Favoured	95.6			
Generously allowed	3.6			
MolProbity score (with H)	2.49			

the crystal consisted of 0.2 *M* bis-tris–HCl pH 6.9, 22%(*w*/*v*) PEG 8000, 1 *M* urea, 15%(*v*/*v*) glycerol, 10%(*w*/*v*) PEG 400, 1 m*M* nonyl β-D-glucoside. The crystal belonged to space group *C*2, with unit-cell parameters *a* = 228.2, *b* = 77.5, *c* = 72.0 Å, α = 90.0, β = 100.9, γ = 90.0°. Data sets were collected at 90 K using a Rayonix MX-225HE CCD detector supported by NSSRC on the BL44XU beamline at SPring-8, Hyogo, Japan. All data were processed with the *HKL*-2000 software package (Otwinowski & Minor, 1997).

2.4. Structure determination

Owing to the conformational flexibility of importin β, we could not obtain a convincing solution using the molecular-replacement method. Initial phase information was derived from the multiple-wavelength anomalous signal of the Zn atoms in the four C2H2-type ZF domains in a 3.45 Å resolution data set. At this stage, we could find electron density for importin β and partially interpret that of Snail1. After manual fitting of each heat repeat (HEAT) of importin β, rigid-body refinement was carried out for the initial model building of importin β using a model of human importin β (PDB entry 1qgk; Cingolani *et al.*, 1999). For model building of Snail1 Z, a 2.5 Å resolution native data set was used. Rigid-body refinement of an importin β model from the 3.45 Å resolution data set followed by successive manual model building led to clearer ZF electron density. Initial C2H2-type ZF models were obtained from the Protein Data Bank (PDB) and also from the Zn-atom sites from the MAD phasing results. Phasing was performed with the *PHENIX* program suite (Adams *et al.*, 2010). Model building and refinement were achieved using *Coot* (Emsley *et al.*, 2010) and *PHENIX*. The refinement converged well to an R_{work} of 22.6% and an R_{free} of 27.2%. The quality and stereochemistry of the refined structure were evaluated using *PROCHECK* (Laskowski *et al.*, 1993) from *CCP*4. 95.2, 4.1 and 0.8% of the amino-acid residues are in the favoured, allowed and outlier regions, respectively. A summary of the crystallographic data and refinement statistics is given in Table 1.

2.5. Binding assay

Owing to the instability of the Snail1 ZF proteins, a pull-down binding assay with purified protein was not adequate to show the binding pattern between wild-type Snail1 ZF (or its mutants) and importin β. Cultured cells expressing wild-typr Snail or its mutant and importin β were mixed in a 2:1 molar ratio (approximately 150 µg Snail1:120 µg importin β) at protein-expression levels. The mixed cells were lysed with 10 ml lysis buffer (20 m*M* Tris–HCl pH 7.4, 300 m*M* NaCl, 1 m*M* DTT, 0.1 m*M* PMSF) by sonication on ice. The supernatant was incubated with 300 µl Phenyl Sepharose beads (GE Healthcare) for 30 min at room temperature. The beads were washed with wash buffer (20 m*M* Tris–HCl pH 7.4, 150 m*M* NaCl, 1 m*M* DTT) and eluted with 5 ml pure water. Each elution sample was concentrated tenfold using concentration tubes (Amicon) and the samples were analyzed by SDS–PAGE.

Snail ZF-GFP and ZF(2–4) mutant binding assays were performed to compare the peak positions of the Snail1–importin β complex by size-exclusion chromatography (SEC) on a Superdex 200 16/600 column. The purified proteins were mixed in a 1:5 stoichiometry (0.0048 m*M* importin β:0.024 m*M* Snail1 mutants) and loaded onto an SEC column pre-equilibrated with 20 m*M* Tris pH 7.4, 50 m*M* NaCl, 1 m*M* DTT. For control experiments, the same quantities of Snail1 mutants were loaded onto the SEC column. The highest peak was collected, concentrated 50-fold using an Amicon tube and analysed by SDS–PAGE.

To estimate the binding affinity of C2H2 ZFs with a variety of C-terminal tails, we attempted pull-down assays or SEC with other long-tailed C2H2 ZF proteins, but these failed owing to poor overexpression and instability of the proteins.

2.6. CD spectrum analysis

Wild-type GST-Snail and mutants were purified in 20 m*M* Tris–HCl pH 7.4, 50 m*M* NaCl, 10 m*M* GSH. To reduce the

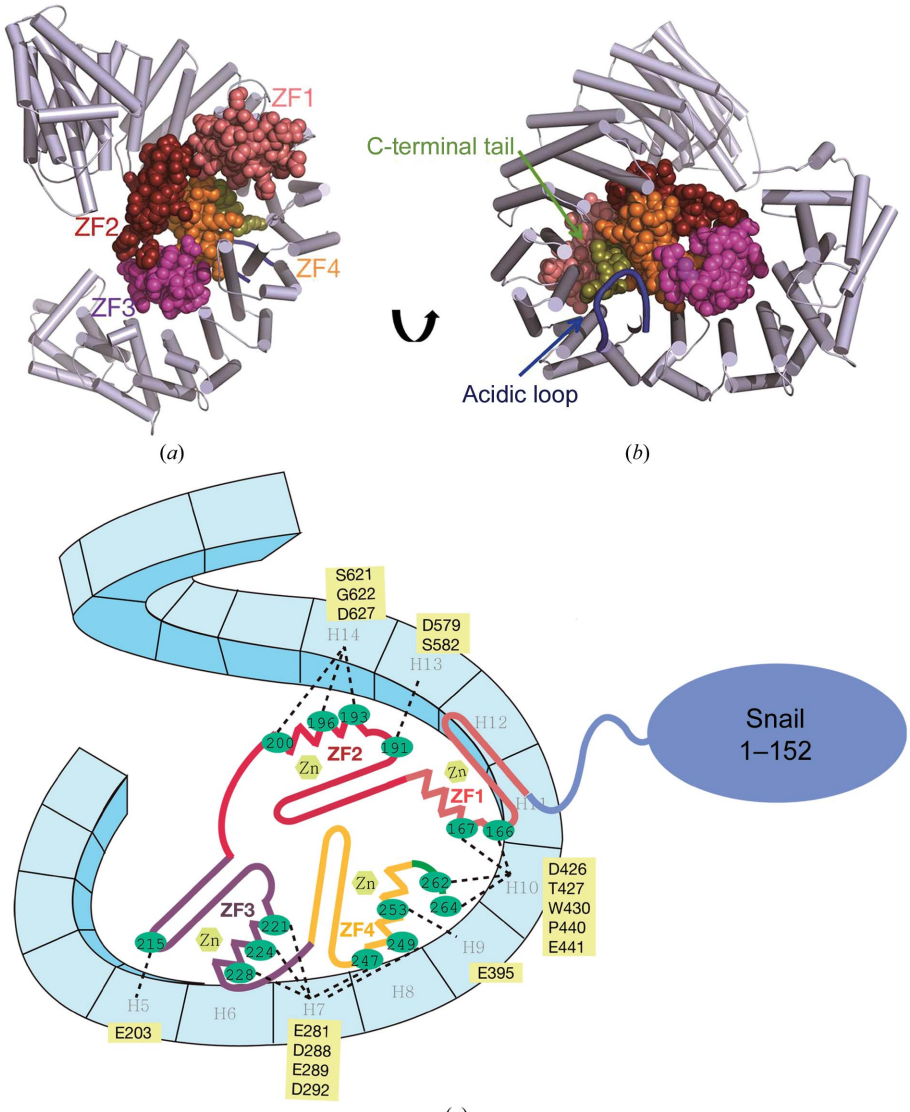

Figure 1
The overall structure of the Snail1 ZF–importin β complex. (*a*) The structure shows four ZFs of human Snail1 (ZF1, salmon; ZF2, red; ZF3, pink; ZF4, orange; C-terminal tail, green) bound to importin β (grey). (*b*) A rotated view of the complex. The conserved acidic loop of importin β is represented in blue. (*c*) Schematic drawing of the complex. ZF1 is on the loop of importin β HEAT10 (H10) and ZF2–ZF4 are captured in the inner surface of importin β. Snail NLSs for importin β are depicted as green balls. Dashed lines between two molecules represent interactions between them. Figs. 1(*a*), 1(*b*) and 2 were prepared using *PyMOL* (Schrödinger).

concentration of GSH, protein samples were diluted to 2 mg ml^{-1} (0.05 m*M* GSH concentration) in 20 m*M* Tris–HCl pH 7.4, 50 m*M* NaCl. Analysis was performed with a CD spectrophotometer (Jasco) in triplicate for each sample.

2.7. Import assay

Synchronized HeLa cells grown on glass cover slips were treated with digitonin (40 µg ml^{-1}) for 5 min. After washing twice with TB buffer [20 m*M* HEPES pH 7.5, 110 m*M* potassium acetate, 5 m*M* magnesium acetate, 250 m*M* sucrose, 0.5 m*M* ethylene glycol-bis(β-aminoethylether)-*N*,*N*,*N*′,*N*′-tetraacetic acid (EGTA)], the permeabilized cells were incubated with ATP working solution (11 m*M* ATP, 50 m*M* phosphocreatine, 300 U ml^{-1} creatine phosphokinase) containing 0.4 µg importin β–GST-Snail1 ZF (or mutant) complex at 30°C for 5 min. For immunofluorescence microscopy to detect GST-fused proteins, the cells were fixed in 3.7% formaldehyde for 15 min at room temperature, permeabilized with 0.5% Triton X-100 for 5 min and then incubated with primary GST antibodies (Santa Cruz Biotechnology) followed by secondary antibodies according to the manufacturers' protocols. Images were captured using a Cool SNAP CCD camera (Roper Scientific) and *Openlab* software (Improvision).

3. Results

3.1. Overall structure of the Snail1 ZF–importin β complex

The X-ray structure of the complex between four ZF domains of human Snail1 (residues 153–264) and full-length human importin β was solved and is presented in Figs. 1 and 2. The Snail1–importin β complex exhibits a superhelical domain with dimensions of 105 × 75 × 60 Å. The structure was refined to an R_{work} of 22.6% and an R_{free} of 27.2% (PDB entry 3w5k). Residues 15–487 and 490–876 of importin β, residues 154–204 and 207–264 of Snail1 and 60 water molecules were included in the final model (Table 1).

Snail1 ZF domains consist of three classical Cys–Cys···His–His (C2H2)-type ZFs and a fourth ZF that contains cysteine as the final zinc-chelating residue, Cys–Cys···His–Cys (C2HC) type, which folds into the same structure as C2H2. The local conformation of each ZF domain in Snail1 showed the same fold as the $\beta\beta\alpha$ structure (Klug, 2010). 15 residues of Snail1, two residues in ZF domain 1 (ZF1), four in ZF domain 2 (ZF2), four in ZF domain 3 (ZF3), three in ZF domain 4 (ZF4) and two C-terminal residues, are evenly involved in the intermolecular interaction with 16 residues of the importin β heat repeats (HEATs) 5–14, out of a total of 19 HEATs, in complex formation (Figs. 1 and 2). The N-terminal area of the ZF1 α-helix is placed in the cleft created by a loop in the short HEAT 10, which is surrounded by the long helices of HEAT 9 and HEAT 11 (Fig. 2*b*, salmon). In ZF1, a hydrophobic interaction between Leu166 of Snail1 and Pro440 of importin β HEAT 10 stabilizes the local conformation, and the weak electron density suggests the possibility that the main-chain N atom of

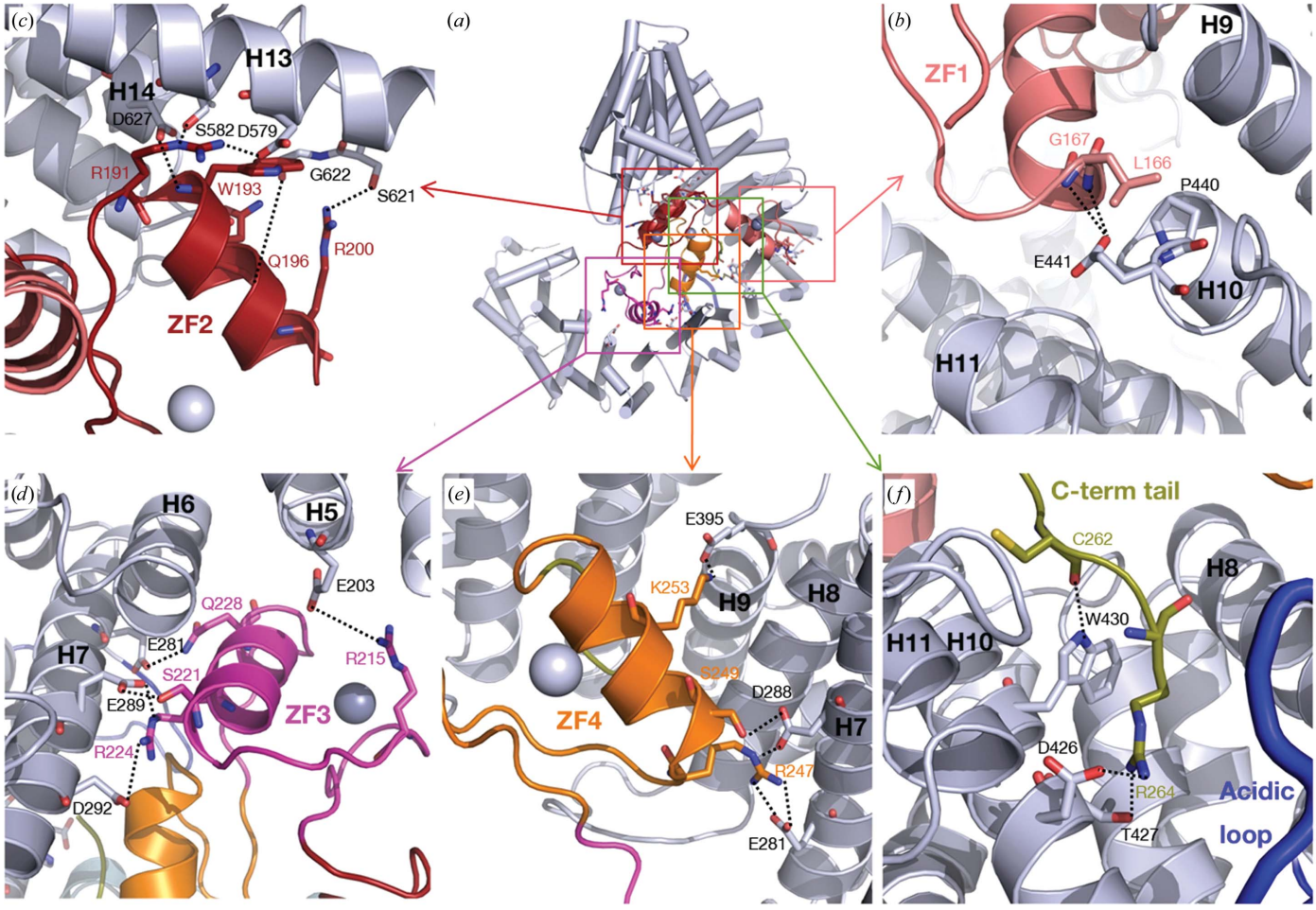

Figure 2
The detailed interactions in the Snail1 ZF–importin β complex. (*a*) The overall interaction between the two proteins is represented in detail. The Snail NLS and interacting importin β residues are presented as a line model. The colour code is the same as that in Fig. 1. (*b*–*f*) The detailed interactions in the binding sites at (*b*) ZF1, (*c*) ZF2, (*d*) ZF3, (*e*) ZF4 and (*f*) the C-terminal tail are displayed in the same colours as in Fig. 1. For the sake of convenience, each figure was rotated from the original view in (*a*).

Gly167 interacts with the carboxyl group of Glu441 of importin β. Three ZFs, ZF2–ZF4, were wound into a ball for the compact and tight interaction with importin β (Fig. 1). In ZF2 (Fig. 2*c*, red), the side chain of Arg191, the main-chain N atom of Trp193, the main-chain O atom of Gln196 and the side chain of Arg200 are involved in hydrogen bonding to the side chains of both Ser582 and Asp579, the side chain of Asp627, the main-chain O atom of Gly622 and the side chain of Ser621, respectively, of importin β HEATs 13–14 (Fig. 2*c*). In ZF3 (Fig. 2*d*, pink), the α-helix of ZF3 is arranged with the inner α-helix of HEAT 6 in an antiparallel direction, which stabilizes complex formation. The side chains of Arg215, Ser221, Arg224 and Gln228 interact with the acidic inner side residues Glu203, Glu289, Asp292 and Glu281, respectively, of importin β HEATs 5–7 (Fig. 2*d*). In ZF4, the side chains of Arg247, Ser249 and Lys253 interact with the carboxyl groups of Glu281, Asp288 and Glu395, respectively, of importin β HEATs 7 and 9 (Fig. 2*e*, orange). The electron density of the C2HC-type ZF4 area is relatively clear compared with the other ZF areas. C2HC-type ZFs are often involved in protein–protein interaction with other proteins (Matthews *et al.*, 2000). In the two C-terminal tail residues, the main-chain amide group of Cys262 interacts with the indole-ring amide of Trp430, and the side chain of Arg264 interacts with the side chains of Asp426 and Thr427 of importin β HEAT 10 (Fig. 2*f*, green).

Owing to the wound conformation of Snail1 ZFs ZF2–ZF4, two intramolecular interactions between ZF2 and ZF4, a hydrogen bond between the side-chain NH_2 group of ZF2 Arg200 and the main-chain O of ZF4 Gln239 and an interaction between the side-chain N atom of ZF2 Trp193 and the main-chain O of ZF4 Ala240, are created (Supplementary Fig. S1[1]).

3.2. Nuclear translocation of Snail family proteins

To analyze the contributions of the 15 residues identified for the nuclear import of Snail1, we prepared 13 point-mutant proteins on the basis of the X-ray structure and carried out a pull-down binding assay (Fig. 3*a*). In order to check the

[1] Supporting information has been deposited in the IUCr electronic archive (Reference: YT5062).

stability of the protein upon mutation, we carried out circular-dichroism (CD) spectroscopic analysis of purified wild-type and mutant GST-Snail1. The CD spectra of the mutants showed a similar pattern to that of the wild-type protein, indicating that the mutated proteins have a properly folded secondary structure (Fig. 3*c*). The single-amino-acid mutants R191E (ZF2), W193A (ZF2), R224E (ZF3) and R247E (ZF4) (Fig. 3*a*, lanes *C*, *D*, *E* and *G*) showed reduced complex-formation ability compared with the wild-type ZF motif. In particular, the combined mutants in multiple ZF domains, R191E/W193A/Q196A/R224E/Q228A (lane *M*), R191E/W193A/Q196A/R247E (lane *N*) and R191E/W193A/Q196A/R224E/Q228A/R247E (lane *O*), completely lost binding ability. Mingot and coworkers predicted the Snail1 NLS using Snail1 ZF mutants which were generated from a three-dimensional model using the six-zinc-finger Aart polypeptide (Mingot *et al.*, 2009). The effective mutants M3 (K187E/R191E) and M9 (R220E/R224E) also contained the structure-derived NLS residues Arg191 and Arg224.

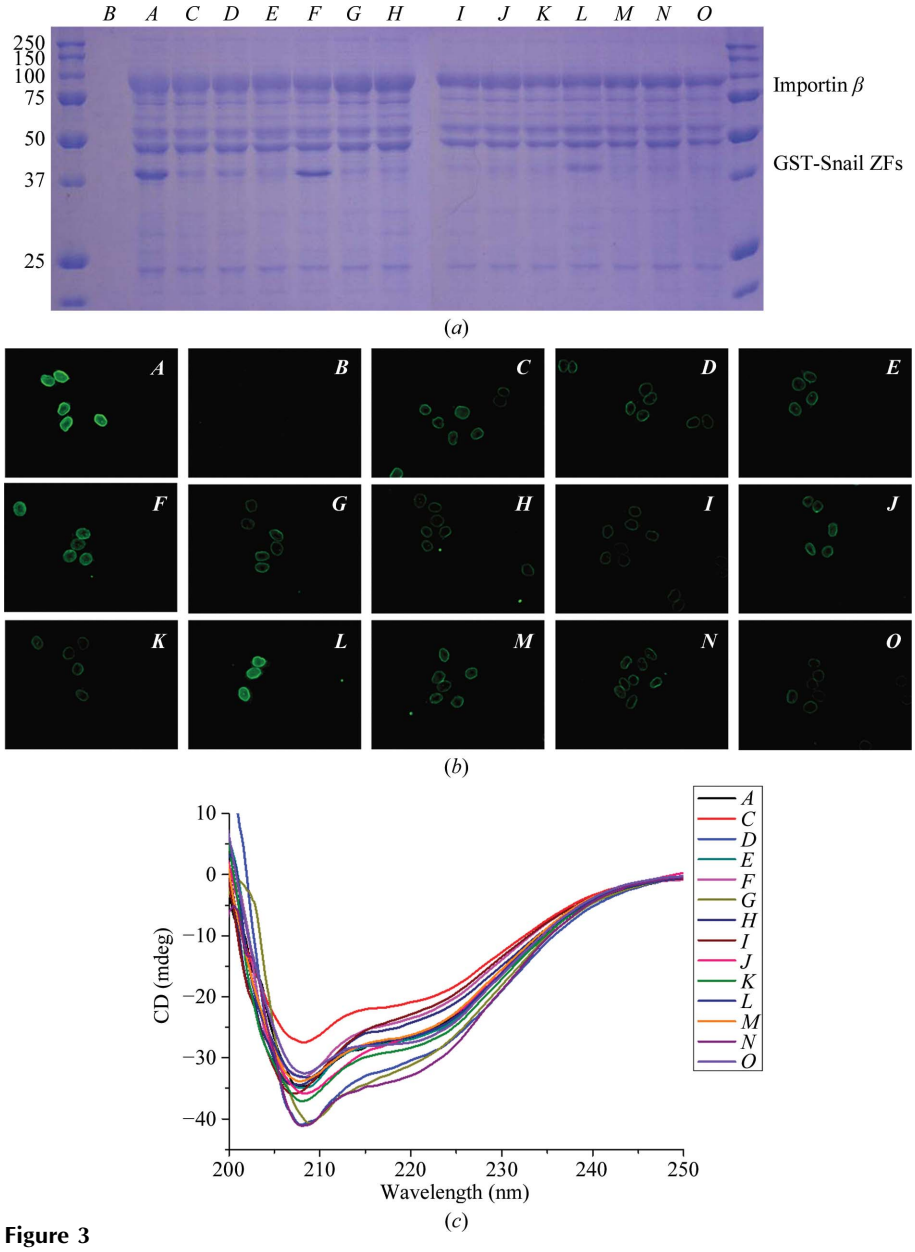

Figure 3
Pull-down binding and nuclear transport assay of the 13 structure-based Snail1 NLS mutants. (*a*) An importin β pull-down binding assay by fixing importin β to Phenyl Sepharose beads was performed with GST-Snail1 ZF and mutants. *A*, Wild-type Snail ZF; *B*, control (Snail ZF only; no importin β); *C*, R191E; *D*, W193E; *E*, R224E; *F*, Q228A; *G*, R247E; *H*, R191E, W193A; *I*, R191E, W193A, Q196A; *J*, R224E, Q228A; *K*, R243E, R247E, K253E; *L*, 153–261; *M*, *I* + *J*; *N*, *I* + *G*; *O*, *I* + *J* + *G*. The leftmost and rightmost lanes contain markers (labelled in kDa). (*b*) Nuclear accumulation of exogenously injected wild-type and mutant Snail1 in digitonin-permeabilized cells. Purified GST-Snail was inserted into the outside of the nucleus of HeLa cells. As in (*a*), *B* represents the control (Snail ZF only). *A* and *C*–*O* represent wild-type or the same Snail ZF mutants as in (*a*) with importin β. (*c*) The CD spectra of the indicated wild-type and mutant GST-Snail1 ZF proteins do not display significant differences.

To confirm the role of each residue of Snail1 in nuclear import, digitonin-permeabilized cell-based *in vitro* transport assays were performed using the above-described recombinant Snail mutant proteins. GST-tagged Snail1 and its mutants were co-transfected with importin β and detected with GST antibody (Fig. 3*b*). Snail1 ZF mutants which have weak binding affinity to importin β showed low nuclear import activity, whereas wild-type Snail1 ZF translocated into the nucleus efficiently. The *in vitro* pull-down binding-assay results were precisely reflected in the digitonin-permeabilized cell experiment. Taken together, the results of our pull-down binding assay and digitonin-permeabilized cell experiments using structure-based mutants reflect the X-ray structural analysis results, indicating that all of the Zn fingers are necessary for efficient nuclear translocation of Snail1 by importin β.

3.3. Importin β grasps Snail1 ZF in a novel mode

The central part of importin β, HEATs 5–14 of a total of 19 HEATs, packs four ZF domains in the concave inner acidic surface using the inherent superhelical conformation of the importin β family proteins. The shape of the Snail ZFs in the X-ray structure of the Snail1 ZF–importin β binary complex is reminiscent of a round snail, with ZF1 as the head, ZF2–ZF4 as the shell and the five C-terminal amino acids as a short tail (Fig. 1). Importin β binds a bundle of four ZFs as if the round snail is held in the palm of a hand (Fig. 1*c*). The interaction between importin β and Snail1 ZFs are

essentially hydrophilic, supported by a lesser number of hydrophobic interactions (Fig. 2). Importin β contacts Snail1 broadly at its inner surface (2205 Å^2), which is comparable in area to the contact areas of the importin β–RanGTP (Lee *et al.*, 2005; 2159 Å^2), importin β–IBB (Cingolani *et al.*, 1999; 1899 Å^2) and importin β–SREBP2 (Lee *et al.*, 2003; 1355 Å^2) binding interfaces. Importin β folds the four Snail ZF domains, which are larger than other NLSs such as IBB (a loop–helix) and SREBP2 (a helix–loop–helix dimer) (Supplementary Fig. S3). Therefore, the superhelical conformation of importin β in the Snail1–importin β complex structure represents a looser helicoidal pitch to accommodate a bulky NLS than those of other importin β–cargo complexes (Supplementary Fig. S4). The location of NLS binding in the importin β molecule is spread over a broad range of HEATs (5–14). The interaction zone of importin β differs from those of other cargoes such as IBB and SREBP2, whose binding sites extend over the central domain to the C-terminal domains of importin β: HEATs 7–19 in the case of IBB and HEATs 7–18 in the case of SREBP2. The specific residues of importin β which interact with Snail1 differ from those of other cargoes such as IBB and SREBP2 when complexed with importin β. The 16 scattered amino acids of importin β are used for accommodation of the Snail1 ZFs as a nonclassical NLS. The numbers of importin β residues used for NLS recognition are 29 and 16 amino acids in the cases of IBB and SREBP2, respectively, while the number of overlapping residues of importin β used for binding both Snail1 and IBB is six and that for both Snail1 and SREBP2 is just one. These results indicate that the binding site of importin β to the various cargoes expands over quite a wide range and show that there is a high degree of overlap in the acidic inside surface of importin β, although the details of the residues of importin β involved in importin β–cargo complex formation are quite different.

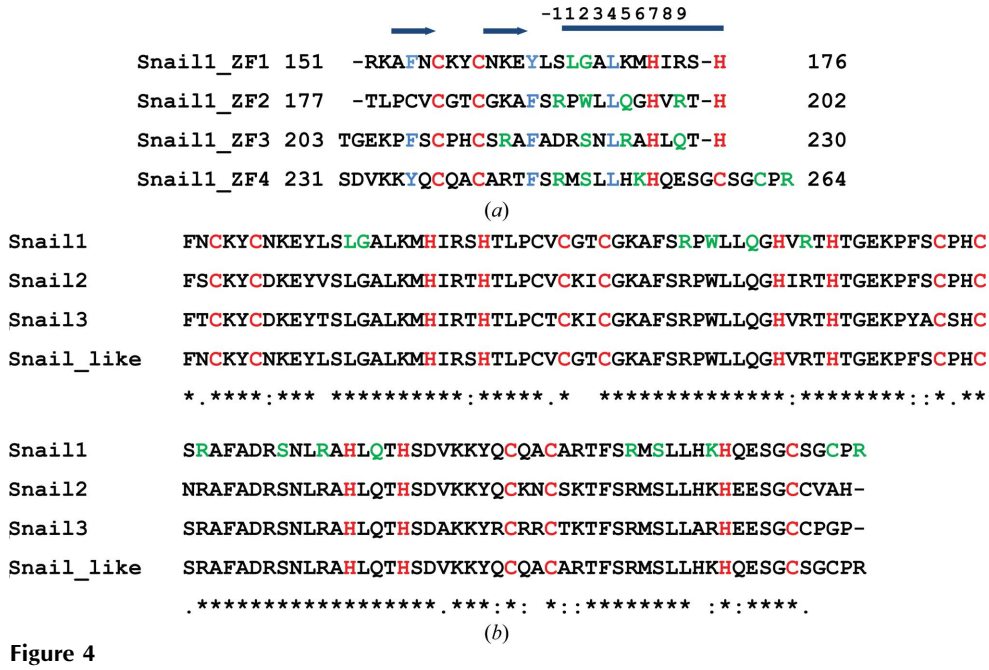

Figure 4
Sequence alignment of Snail1 ZFs and Snail family proteins. (*a*) Structure-based sequence alignment of Snail1 ZF residues 151–264. C–C···H–H (C2H2) ZFs are coloured red and the conserved Phe1, Phe2 and Leu are coloured light blue. The NLS residues are represented in green. (*b*) Sequence-alignment results for the ZF domains of Snail family proteins (Snail1, NM_005985.3; Snail2, NM_003068; Snail3, NM_178310.3; Snail-like, EAW70471.1) indicate that the ZF domains are highly conserved.

3.4. Snail1 ZF in protein–protein interaction

The X-ray structure of Snail1–importin β reveals that the Snail1 NLS residues binding to importin β are not restricted to the DNA-recognition residues of the ZF domain in helical positions −1, 2 and 6, but are expanded to positions 1, 5 and 9, which are new protein–protein interaction (PPI) sites (Fig. 4*a*, coloured green). The opposite surfaces of the His–His Zn-chelating site in the α-helix of $\beta\beta\alpha$ ZF domains are mainly involved in Snail1–importin β complex formation (Fig. 5*a*). Generally, a C2H2 ZF protein interacts with a 3 bp subsite on one strand of the DNA using the amino-acid residues in helical positions −1, 3 and 6 and with position 2 on the other strand of the DNA; these residues are located around the N-terminus of the α-helix (Klug, 2010). In addition to Cys–Cys···His–His, the classical C2H2 ZF also contains three other conserved hydrophobic residues: Phe1 (or Tyr), Phe2 and Leu (Fig. 4*a*; all coloured light blue). NLS residues for importin β recognition are intensively located between the conserved Phe2 and the first His of the ZF His–His. The ZF3 domain has two characteristic NLS residues, Gln228 and Arg215, distant from the N-terminus of the α-helix. Although the Zn-chelating sites are hardly involved in the recognition of importin β, the conspicuous position of Gln228, which is located between His–His Zn-binding residues, is an exception. Gln228 potentiates complex formation by cooperation with Arg247 to interact with Glu281 of importin β. The residue Arg215 on the second β-strand of ZF3 also takes part in the PPI. The two C-terminal short tail residues Cys262 and Arg264 interact with importin β HEAT 10. However, a pull-down binding assay result using a Snail1 mutant with a deletion of the C-terminal tail, the sequence of which is not conserved among the Snail family (Fig. 4*b*), reveals that this interaction is not critical for binding (Fig. 3*a*, lane *L*).

3.5. Selective import of Snail1 by C-terminal tail size

Because the end of the ZF4 α-helix, which is located just under the ZF2 domain, cannot extend to the upper side, the five-amino-acid C-terminal short tail (Figs. 2*a* and 2*f*, green)

orients to the inner surface of importin β, which has a small space and is obstructed by the conserved acidic loop (blue in Figs. 1*b* and 2*a*), which is only adequate to accommodate a few amino acids. The X-ray structure shows that the end of the Snail1 C-terminal tail is blocked by the acidic loop of importin β and the ZF4 domain. Although there are many kinds of C2H2-type ZFs, nuclear import by direct recognition of importin β is observed in a limited number of C2H2-type ZF proteins such as Snail1, Wt1, KLF1 and KLF8, which are terminated by ZF domains with just a few amino acids as a tail (Fig. 5*b*). To evaluate the role of the C-terminal tail in Snail1, we produced Snail ZF-GFP, which has two non-native residues between Snail ZF and GFP. To investigate the complex-formation ability of Snail1 mutants with importin β, we carried out size-exclusion chromatography (SEC). The highest peak fractions of each complex are shown in the right panel and the fractions of Snail ZF, ZF-GFP and ZF(2–4) alone at the same elution volume as the complex are shown on the left as a control (Fig. 6*a*). The SEC results showed that the binding efficiency of the Snail1 ZF-GFP molecule to importin β was extremely low (Fig. 6*a*; Snail ZF-GFP, Output) compared with that of Snail1 ZF to importin β (Fig. 6*a*; Snail ZF, Output). The digitonin-permeabilized cell experiment with the same constructs showed the same result as that from SEC (Fig. 6*b*). This may be explained by the surplus GFP domain after the ZF domains disturbing the efficient binding of Snail1 ZF. Therefore, the importance of the C-terminal tail in Snail C2H2 ZF domains might be related to the selectivity of the Snail family proteins for importin β binding. The Snail1 ZF(2–4) (ZF2–ZF3–ZF4) mutant also showed a binding affinity for importin β on SEC [Fig. 6*a*; Snail ZF(2–4), Output] and a reasonable transport ability in digitonin-permeabilized cells, although it was weaker than that of the four ZFs of Snail1 (Fig. 6*b*).

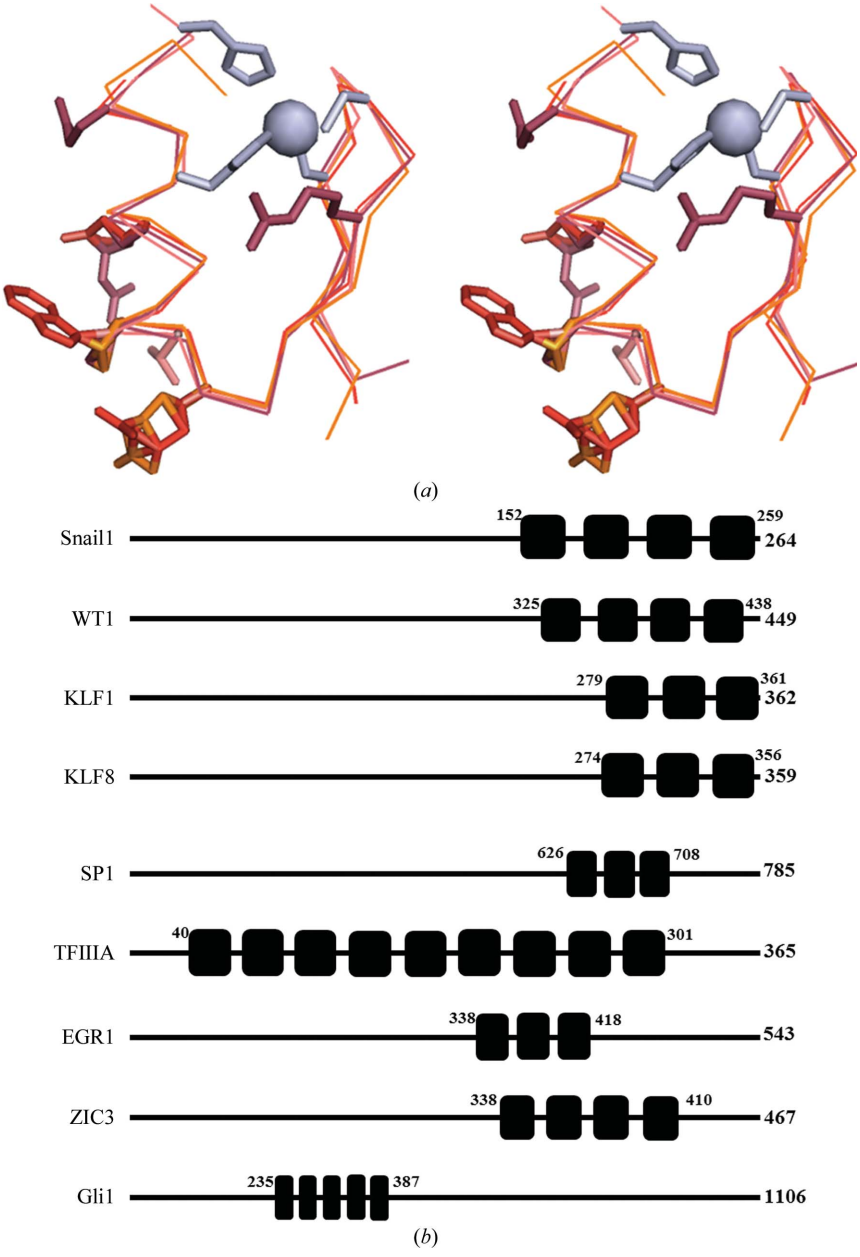

Figure 5
Structure-based alignment of Snail1 ZFs and ZF family proteins. (*a*) R.m.s. fitting results of the four Snail1 ZF domains. The NLS amino acids are represented as wire models. The NLS residues for importin β are concentrated on the opposite surface of the Zn chelating site. (*b*) Snail and other ZF proteins which are known to be transported by their ZF regions are depicted. Snail1, Wt1, EKLF/KLF1 and KLF8 (Wt1, NM_000378; KLF1, NM_006563.3; KLF8, NM_007250) with a short tail are transported by direct binding to importin β, while SP1, TFIIIA, ZIC3 and Gli1 (Sp1, NM_138473.2; TFIIIA, NM_002097.2; ZIC3, NM_003413.3; Gli1, NM_005269.2) with a long tail are known to be transported in an importin α/importin β-dependent manner.

4. Discussion

Here, we report two main findings. Importin β selectively binds Snail ZF protein by the conserved acidic loop in importin β family proteins. This selectivity is important for the biological function of Snail family proteins. Also, we present a novel ZF PPI mode which shows an unusual interaction of ZF domains.

4.1. Structural requirement for C2H2 ZF binding to importin β

From the Snail1 ZF–importin β structure, the four ZF domains are needed for efficient nuclear translocation by importin β directly. Single-amino-acid mutants in ZF2–ZF4 [R191E (ZF2), W193A (ZF2), R224E (ZF3) and R247E (ZF4)] showed highly reduced complex formation and nuclear translocation ability (Fig. 3*a* and 3*b*, lanes *C*, *D*, *E*, *F* and *G*), while the Snail1 ZF(2–4)

(ZF2–ZF3–ZF4) mutant showed a binding affinity to importin β and a reasonable transport ability, although it was weaker than that of the four ZFs of Snail1 (Figs. 6*a* and 6*b*). Although the four ZFs of Snail showed efficient nuclear translocation, the three ZF domains [Snail ZF(2–4)] might be the core for importin β binding, which is required for nuclear import. The nuclear import of KLF1 and KLF8, which contain three consecutive ZFs, occurs by complex formation between their ZF domains and importin β (Pandya & Townes, 2002; Quadrini & Bieker, 2002; Mehta *et al.*, 2009). From the result of sequence alignment, the three ZFs of KLF1 and KLF8 match the ZF2–ZF4 domains of Snail1, although the NLS residues are not conserved (Supplementary Fig. S2).

Because the short tail (five amino acids) of the end of ZF4 in Snail1 is located in a space which is too narrow to accept over a dozen tail amino acids, a long-tailed ZF protein after the last ZF domain may have difficulty in binding importin β efficiently owing to structural restriction in the conserved acidic loop of importin β (Figs. 1*b* and 2*f*). The secondary-structure prediction of the long-tailed ZF proteins showed that they have a helical structure 5–20 amino acids after the final ZF domain. This helical structure may disturb the binding of long-tailed ZF proteins by importin β. We constructed Snail1 ZF-GFP, which has two amino acids between Snail ZF and GFP, to evaluate the effect of the C-terminal tail length in Snail1. In Snail binding to importin β, the acidic loop acts as a selection tool for short-tailed ZF cargoes, which differs from the general usage of the acidic loop, in which the acidic loop forms part of a mutually exclusive binding site which accepts either cargo or RanGTP (Conti *et al.*, 2006). SEC results showed that the binding efficiency of the Snail1 ZF-GFP molecule to importin β was very low compared with that of Snail1 ZF to importin β (Fig. 6*a*). The GFP domain disturbs the proficient binding of Snail1 ZFs owing to a clash with the acidic loop. The results of the digitonin-permeabilized cell experiment were in agreement with those of SEC (Fig. 6*b*). In humans, there are many C2H2 ZF proteins; they have been estimated to comprise as many as 3% of the genes coding for C2H2 proteins (Bateman *et al.*, 2002). C2H2-type ZF proteins, such as Snail1, Wt1 (Depping *et al.*, 2012), EKLF/KLF1 (Pandya & Townes, 2002; Quadrini & Bieker, 2002), KLF8 (Mehta *et al.*, 2009), Gli (Hatayama & Aruga, 2012), Zic3 (Bedard *et al.*, 2007), SP1 (Ito *et al.*, 2010), Zif268 (Shields & Yang, 1997), Zac1 (Huang *et al.*, 2007), Znf131 (Donaldson *et al.*, 2007) and TFIIIA (Wischnewski *et al.*, 2004), are known to be transported to the nucleus by their consecutive ZF regions (Fig. 5*b*). Knowledge of the nuclear transport factor for a specific ZF protein is meaningful in order to understand the nuclear transport mechanism. Among these proteins, Snail1, Wt1, KLF1 and KLF8 are transported by importin β directly, while Gli, Zic3, SP1, Znf131, Zif268, Zac1 and TFIIIA are known to be transported in an importin α/importin β-dependent manner. Interestingly, Snail1, Wt1, KLF1 and KLF8 are commonly terminated by ZF

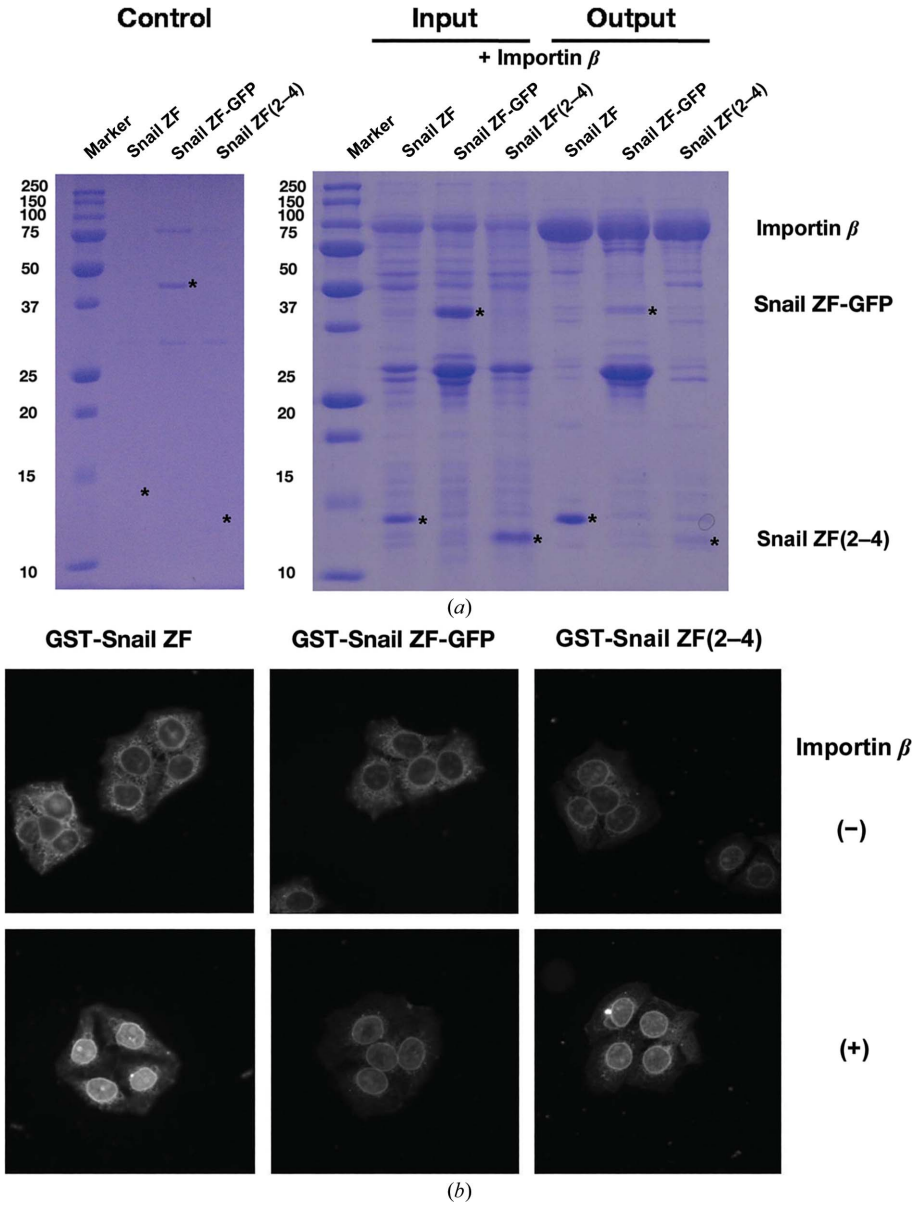

Figure 6
Binding and nuclear transport assay of Snail ZF, Snail ZF-GFP and Snail1 ZF(2–4) mutant. (*a*) The size-exclusion chromatography (SEC) results for Snail ZF, Snail1 ZF-GFP and Snail1 ZF(2–4) alone or with importin β are shown on SDS–PAGE. The size-exclusion chromatograms are presented in Supplementary Fig. S5. (*b*) Nuclear accumulation of exogenously injected Snail ZF, Snail1 ZF-GFP and Snail1 ZF(2–4) in digitonin-permeabilized cells.

domains with short tails, while Gli, Zic3, SP1, Znf131, Zif268, Zac1 and TFIIIA have a long tail after the ZF domains (Fig. 5*b*). Therefore, the tail size after the ZF domain may be a factor for cargo selection by importin β on the assumption that the ZF domains of various ZF proteins interact with importin β in the same way as Snail1 does. The Snail protein is highly unstable because of tight regulation by the ubiquitin–proteasome pathway, with a half-life of 25 min (Zhou *et al.*, 2004). Thus, transcriptional regulation by Snail1 should occur in a rapid manner. In nuclear translocation of Snail, direct nuclear import by importin β might be a rapid process for the unstable protein Snail.

4.2. Protein–protein interaction (PPI) between Snail ZF and importin β

The PPI sites in the C2H2-type ZF domain are interesting because the positions involved in C2H2-type ZF PPI have been little studied owing to the limited structural information on C2H2-type ZF protein complexes determined at atomic resolution (Liew *et al.*, 2005). The C2H2-type and C2HC-type ZFs share similar structures, but they have different functions. While C2H2-type ZFs are generally involved in DNA or RNA binding, the C2HC-type ZFs interact with other proteins (Matthews *et al.*, 2000). In Snail–importin β complex formation, the Snail C2HC-type ZF4 also showed a strong binding affinity for importin β compared with other Snail ZFs. The Snail1 ZF NLS is mainly located in the broad α-helix region with a residue on the second β-sheet in our X-ray structure (Fig. 1*c*). C2H2-type ZF proteins were originally identified as DNA-binding domains strictly confined to helical positions -1, 3 and 6 and position 2 on the other strand of the DNA (Liew *et al.*, 2005; Fig. 4*a*). However, for PPI in the case of the Snail ZF–importin β complex, the binding site has spread to helical positions -1, 1, 2, 5, 6 and 9, which represents greater diversity than the DNA-binding mode (Figs. 1*c* and 4*a*). As shown in Fig. 5(*a*), the NLS residues are mainly located on the opposite surface to the Zn-chelating side. The Snail ZF–importin β complex could not simultaneously bind DNA, since Snail uses the α-helix of the C2H2-type ZF domain for binding importin β and DNA. However, Liew and coworkers demonstrated that the ZF–ZF PPI site is different from the DNA–ZF binding site by showing that two ZF-domain associations by GATA-1–FOG PPI simultaneously occur on FOG–DNA complex formation (Liew *et al.*, 2005). The unusual positions Arg215 and Gln228, which are located on the second β-strand and the C-terminal area of the α-helix, respectively, are also involved in PPI. The conserved phenylalanine or isoleucine in Snail ZF is not used for binding to importin β.

4.3. Conformational change of Snail ZFs upon complex formation with importin β

The tight conformation of ZFs created by the intramolecular interaction between ZF2 and ZF4 in the Snail1–importin β complex is unlikely to be the same as the conformation of uncomplexed Snail1 ZF, considering the linear conformation of the adjacent ZFs in DNA–ZF complexes. Although the distance between ZF2 and ZF4 is not great within the Snail1–importin β structure, owing to the wound conformation of ZF2–ZF4, there are just two hydrophilic interactions between two ZFs at a distance of 3.5 Å, between Arg200 and Gln239 and between Trp193 and Ala240, without any hydrophobic interaction. The compact shape of Snail1 ZF2–ZF4 induced by complex formation could not be sustained without the help of importin β, which stabilizes the high tension around ZFs by rolling them up. From the interaction between the FOG ZF1 and GATA-1, a specific C2H2 ZF is capable of mediating PPI with a low binding affinity, with an weak association constant of $4.5 \times 10^4\ M^{-1}$ (Liew *et al.*, 2005), which is similar to the interaction between ZF2 and ZF4 in our structure that showed two hydrophilic interactions.

4.4. Nuclear translocation mechanism of Snail

The *in vitro* digitonin-permeabilized transport assay in HeLa cells indicates that the nuclear translocation patterns of GST-Snail1 ZF mutants coincide with the pull-down assay results of GST-Snail1 ZF with importin β (Fig. 3*a*). The ZF domains of the Snail family proteins Snail1 ZF1–ZF4, Snail2 ZF2–ZF5 and Snail3 ZF2–ZF5 are strongly conserved at the amino-acid level, ranging from 80 to 87% (Fig. 4*b*). In particular, the NLS residues of Snail1 ZF1–ZF4 are conserved in all Snail family members, suggesting that nuclear import of Snail family proteins might occur by the recognition of ZF domains by importin β. The subcellular localization and activity of Snail1 is regulated by phosphorylation. Phosphorylation of Snail1 on Ser246 by p21-activated kinase (Pak1) induces accumulation of Snail1 in the nucleus and then potentiates the transcriptional repression functions of Snail (Yang *et al.*, 2005). A S246A substitution in Snail1 or Pak1 knockdown by short interference RNA blocked Pak1-mediated Snail1 phosphorylation, leading to increased cytoplasmic accumulation of Snail and attenuation of Snail repressor activity in breast cancer cells (Yang *et al.*, 2005). However, the phosphorylation of Ser246 may not affect the binding of Snail1 to importin β, since Ser246 is located in the loop area before the ZF4 α-helix which is in an open space in the Snail1–importin β complex structure. Therefore, the mechanism of cytoplasmic accumulation of the S246A mutant may result in the efficient nuclear export of Snail1 by an unknown regulation mechanism. Ser246 and surrounding amino acids are conserved in Snail1, Snail2 and Snail3, but not in Scratch proteins, suggesting that the post-translational regulation of Snail Ser246 by Pak1 is specific to the Snail family (Yang *et al.*, 2005). Recently, another phosphorylation of Snail1 at Thr203 by Lats2 was found to occur in the nucleus and to retain Snail1 in the nucleus, thereby enhancing protein stability and function (Zhang *et al.*, 2012). Based on the X-ray structure, the phosphorylation of Thr203, which is located at the end of the second ZF domain α-helix, may not disturb the formation of the nuclear import complex with importin β. Therefore, nuclear accumulation of Snail1 by Thr203 phosphorylation may occur through a number of possibilities, including the

alteration of the Snail1 binding affinity to the nuclear export machinery or to other nuclear proteins.

In summary, the conserved acidic loop in importin β acts as a selection tool for specific ZF proteins among the various ZF proteins that might be important for prompt nuclear import of a fragile Snail protein. In addition, a novel PPI in the ZF protein gives an indication of a new usage of ZF proteins.

This research was supported by a National Research Foundation of Korea (NRF) grant funded by the Korean Government (MEST) (2011-0017405). We would like to acknowledge Professor Tomitake Tsukihara and Professor Atsushi Nakagawa for their invaluable discussion and support. The synchrotron-radiation experiments were performed on BL44XU of SPring-8 with the approval of the Japan Synchrotron Radiation Research Institute (JASRI) and the Protein Beamline at Pohang Light Source, Republic of Korea.

References

Adams, P. D. *et al.* (2010). *Acta Cryst.* D**66**, 213–221.
Bateman, A., Birney, E., Cerruti, L., Durbin, R., Etwiller, L., Eddy, S. R., Griffiths-Jones, S., Howe, K. L., Marshall, M. & Sonnhammer, E. L. (2002). *Nucleic Acids Res.* **30**, 276–280.
Batlle, E., Sancho, E., Francí, C., Domínguez, D., Monfar, M., Baulida, J. & García De Herreros, A. (2000). *Nature Cell Biol.* **2**, 84–89.
Bedard, J. E., Purnell, J. D. & Ware, S. M. (2007). *Hum. Mol. Genet.* **16**, 187–198.
Cano, A., Pérez-Moreno, M. A., Rodrigo, I., Locascio, A., Blanco, M. J., del Barrio, M. G., Portillo, F. & Nieto, M. A. (2000). *Nature Cell Biol.* **2**, 76–83.
Choi, S., Song, J., Son, S.-Y., Park, I. Y., Yamashita, E. & Lee, S. J. (2013). *Acta Cryst.* F**69**, 1049–1051.
Cingolani, G., Petosa, C., Weis, K. & Müller, C. W. (1999). *Nature (London)*, **399**, 221–229.
Conti, E., Müller, C. W. & Stewart, M. (2006). *Curr. Opin. Struct. Biol.* **16**, 237–244.
De Craene, B., Gilbert, B., Stove, C., Bruyneel, E., van Roy, F. & Berx, G. (2005). *Cancer Res.* **65**, 6237–6244.
Depping, R., Schindler, S. G., Jacobi, C., Kirschner, K. M. & Scholz, H. (2012). *Cell. Physiol. Biochem.* **29**, 223–232.
Domínguez, D., Montserrat-Sentís, B., Virgós-Soler, A., Guaita, S., Grueso, J., Porta, M., Puig, I., Baulida, J., Francí, C. & García de Herreros, A. (2003). *Mol. Cell. Biol.* **23**, 5078–5089.
Donaldson, N. S., Daniel, Y., Kelly, K. F., Graham, M. & Daniel, J. M. (2007). *Biochim. Biophys. Acta*, **1773**, 546–555.
Emsley, P., Lohkamp, B., Scott, W. G. & Cowtan, K. (2010). *Acta Cryst.* D**66**, 486–501.
Hatayama, M. & Aruga, J. (2012). *Vitam. Horm.* **88**, 73–89.
Huang, S.-M., Huang, S.-P., Wang, S.-L. & Liu, P.-Y. (2007). *Biochem. J.* **402**, 359–366.
Ito, T., Kitamura, H., Uwatoko, C., Azumano, M., Itoh, K. & Kuwahara, J. (2010). *Biochem. Biophys. Res. Commun.* **403**, 161–166.
Klug, A. (2010). *Annu. Rev. Biochem.* **79**, 213–231.
Laskowski, R. A., MacArthur, M. W., Moss, D. S. & Thornton, J. M. (1993). *J. Appl. Cryst.* **26**, 283–291.
Lee, S. J., Matsuura, Y., Liu, S. M. & Stewart, M. (2005). *Nature (London)*, **435**, 693–696.
Lee, S. J., Sekimoto, T., Yamashita, E., Nagoshi, E., Nakagawa, A., Imamoto, N., Yoshimura, M., Sakai, H., Chong, K. T., Tsukihara, T. & Yoneda, Y. (2003). *Science*, **302**, 1571–1575.
Liew, C. K., Simpson, R. J. Y., Kwan, A. H. Y., Crofts, L. A., Loughlin, F. E., Matthews, J. M., Crossley, M. & Mackay, J. P. (2005). *Proc. Natl Acad. Sci. USA*, **102**, 583–588.
Matthews, J. M., Kowalski, K., Liew, C. K., Sharpe, B. K., Fox, A. H., Crossley, M. & MacKay, J. P. (2000). *Eur. J. Biochem.* **267**, 1030–1038.
Mehta, T. S., Lu, H., Wang, X., Urvalek, A. M., Nguyen, K.-H. H., Monzur, F., Hammond, J. D., Ma, J. Q. & Zhao, J. (2009). *Cell Res.* **19**, 1098–1109.
Mingot, J. M., Vega, S., Maestro, B., Sanz, J. M. & Nieto, M. A. (2009). *J. Cell Sci.* **122**, 1452–1460.
Otwinowski, Z. & Minor, W. (1997). *Methods Enzymol.* **276**, 307–326.
Pandya, K. & Townes, T. M. (2002). *J. Biol. Chem.* **277**, 16304–16312.
Peinado, H., Ballestar, E., Esteller, M. & Cano, A. (2004). *Mol. Cell. Biol.* **24**, 306–319.
Peinado, H., Olmeda, D. & Cano, A. (2007). *Nature Rev. Cancer*, **7**, 415–428.
Poser, I., Domínguez, D., de Herreros, A. G., Varnai, A., Buettner, R. & Bosserhoff, A. K. (2001). *J. Biol. Chem.* **276**, 24661–24666.
Quadrini, K. J. & Bieker, J. J. (2002). *J. Biol. Chem.* **277**, 32243–32252.
Sekimoto, T., Miyamoto, Y., Arai, S. & Yoneda, Y. (2011). *J. Biol. Chem.* **286**, 15126–15131.
Shields, J. M. & Yang, V. W. (1997). *J. Biol. Chem.* **272**, 18504–18507.
Stewart, M. (2007). *Nature Rev. Mol. Cell Biol.* **8**, 195–208.
Thiery, J. P. (2002). *Nature Rev. Cancer*, **2**, 442–454.
Thiery, J. P. & Sleeman, J. P. (2006). *Nature Rev. Mol. Cell Biol.* **7**, 131–142.
Wischnewski, J., Rudt, F. & Pieler, T. (2004). *Eur. J. Cell Biol.* **83**, 55–66.
Wu, Y., Evers, B. M. & Zhou, B. P. (2009). *J. Biol. Chem.* **284**, 640–648.
Yamasaki, H., Sekimoto, T., Ohkubo, T., Douchi, T., Nagata, Y., Ozawa, M. & Yoneda, Y. (2005). *Genes Cells*, **10**, 455–464.
Yang, Z., Rayala, S., Nguyen, D., Vadlamudi, R. K., Chen, S. & Kumar, R. (2005). *Cancer Res.* **65**, 3179–3184.
Zhang, K., Rodriguez-Aznar, E., Yabuta, N., Owen, R. J., Mingot, J. M., Nojima, H., Nieto, M. A. & Longmore, G. D. (2012). *EMBO J.* **31**, 29–43.
Zhou, B. P., Deng, J., Xia, W., Xu, J., Li, Y. M., Gunduz, M. & Hung, M.-C. (2004). *Nature Cell Biol.* **6**, 931–940.